ORIGINAL ARTICLE

ORAL DISEASES   WILEY

1-Palmitoyl-2-linoleoyl-3-acetyl-rac-glycerol ameliorates chemoradiation-induced oral mucositis

Solji Choi[1,2] | Su-Hyun Shin[1,2] | Ha-Reum Lee[3] | Ki-Young Sohn[3] | Sun Young Yoon[3] | Jae Wha Kim[1,2]

[1]Division of Systems Biology and Bioengineering, Cell Factory Research Center, Korea Research Institute of Bioscience and Biotechnology, Daejeon, Korea

[2]Department of Functional Genomics, University of Science and Technology, Daejeon, Korea

[3]ENZYCHEM Lifesciences, Jechon-si, Korea

Correspondence
Jae Wha Kim, Cell Factory Research Center, Divisions of Systems Biology and Bioengineering, Korea Research Institute of Bioscience and Biotechnology, 125 Gwahak-ro, Yuseong-gu, Daejeon 34141, Korea.
Email: wjkim@kribb.re.kr

Abstract

Objective: This study was designed to investigate whether necroptosis is involved in the pathogenesis of chemoradiation-induced oral mucositis in a murine model and whether 1-palmitoyl-2-linoleoyl-3-acetyl-rac-glycerol (PLAG) ameliorates this disorder.

Materials and Methods: A chemoradiation-induced oral mucositis model was established by treating mice with concurrent 5-fluorouracil (100 mg/kg, i.p.) and head and neck X-irradiation (20 Gy). Phosphate-buffered saline or PLAG (100 mg/kg or 250 mg/kg, p.o.) was administered daily. Body weights were recorded daily, and mice were sacrificed on Day 9 for tongue tissue analysis.

Results: On Day 9, chemoradiotherapy-treated (ChemoRT) mice had tongue ulcerations and experienced significant weight loss (Day 0:26.18 ± 1.41 g; Day 9:19.44 ± 3.26 g). They also had elevated serum macrophage inhibitory protein 2 (MIP-2) (control: 5.57 ± 3.49 pg/ml; ChemoRT: 130.14 ± 114.54 pg/ml) and interleukin (IL)-6 (control: 198.25 ± 16.91 pg/ml; ChemoRT: 467.25 ± 108.12 pg/ml) levels. ChemoRT-treated mice who received PLAG exhibited no weight loss (Day 0:25.78 ± 1.04 g; Day 9:26.46 ± 1.68 g) and had lower serum MIP-2 (4.42 ± 4.04 pg/ml) and IL-6 (205.75 ± 30.41 pg/ml) levels than ChemoRT-treated mice who did not receive PLAG. Tongue tissues of mice who received PLAG also displayed lower phosphorylation levels of necroptotic signalling proteins.

Conclusion: 1-Palmitoyl-2-linoleoyl-3-acetyl-rac-glycerol mitigated chemoradiation-induced oral mucositis by modulating necroptosis.

KEYWORDS
1-palmitoyl-2-linoleoyl-3-acetyl-rac-glycerol (PLAG), chemoradiation-induced oral mucositis, damage-associated molecular pattern molecules (DAMPs), necroptosis, neutrophils

1 | INTRODUCTION

Oral mucositis is one of the most debilitating complications of common cancer treatments, such as chemotherapy and radiation therapy (Zhang et al., 2012). The overall occurrence of oral mucositis is over 90% in patients with head and neck cancer who received chemoradiotherapy (He et al., 2014; Muanza et al., 2005). Oral mucositis is characterized by acute inflammation and ulcerative lesions in the mucous membranes lining the mouth and throat (Al-Dasooqi et al., 2013; Maria, Eliopoulos, & Muanza, 2017; Sottili et al., 2018).

Regardless of increased efforts for preventing the disorder, treatments are primarily limited to opioid analgesics for pain relief and antibiotics for secondary bacterial infection (Im et al., 2019). Moreover, the mechanism and pathobiology of oral mucositis are not fully understood (Bertolini, Sobue, Thompson, & Dongari-Bagtzoglou, 2017).

Necroptosis is a form of programmed cell death with features of necrosis and apoptosis (Liu et al., 2018). It is an inflammatory cell death involving rapid plasma membrane permeabilization, leading to the release of cell contents and exposure of endogenous molecules, such as damage-associated molecular patterns (DAMPs) (Kaczmarek, Vandenabeele, & Krysko, 2013). Necroptosis occurs through activation of the necroptosis signalling axis, which includes receptor-interacting protein kinase 1 (RIPK1), receptor-interacting protein kinase 3 (RIPK3) and mixed lineage kinase domain-like pseudokinase (MLKL) (Barbosa et al., 2018a).

An increasing number of studies have suggested that necroptosis is associated with various acute injuries in different diseases (Zhao et al., 2015). Further, chemotherapy has been reported to promote inflammatory cell death of epithelial cells, and it has been suggested that necroptosis is induced via a positive feedback loop by elevated inflammatory cytokine levels produced by anti-cancer treatments (Xu et al., 2015). Moreover, an anti-necroptotic agent has shown protective effects against 5-fluorouracil (FU)-induced oral mucositis in a mouse model, acting through regulation of a DAMP known as high-mobility group box 1 (HMGB1) (Im et al., 2019). Therefore, in the current study, we decided to investigate whether necroptosis is associated with chemoradiation-induced oral mucositis.

Necroptotic cells passively release DAMPs. HMGB1 is the DAMP most commonly associated with oral mucositis (Tancharoen, Shakya, Narkpinit, Dararat, & Kikuchi, 2018; Vasconcelos et al., 2016). Interleukin (IL)-6 is also released as a sequela of necroptosis and is known to initiate inflammation in other tissues (Deepa, Unnikrishnan, Matyi, Richardson, & Hadad, 2018; Zhao et al., 2015). IL-6 is an extensively studied proinflammatory cytokine in oral mucositis, and an anti-IL-6 monoclonal antibody has undergone clinical testing for the prevention of oral mucositis (Cinausero et al., 2017). One of the other major features of necroptosis is that it upregulates neutrophil chemoattractant. IL-8 is a chemotactic cytokine for neutrophils, and it is upregulated when necroptosis occurs (de Oliveira et al., 2013; Zhu et al., 2018).

1-Palmitoyl-2-linoleoyl-3-acetyl-rac-glycerol (PLAG) is a monoacetyl diacylglycerol that contains an acetyl group at the third position of the glycerol backbone (Hwang et al., 2015; Jeong et al., 2016). PLAG has been studied for its anti-inflammatory effects and has exhibited therapeutic efficacy against several inflammatory diseases (Kim et al., 2017; Ko et al., 2018). We previously showed that PLAG has therapeutic efficacy against chemotherapy- and scratching-induced oral mucositis in murine models via modulating neutrophil migration (Lee et al., 2016). PLAG was also shown to downregulate several proinflammatory cytokines induced by oral mucositis.

In the current study, we examined whether necroptosis is a contributing factor to chemoradiation-induced oral mucositis and whether PLAG exhibited mitigating effects against this disorder. We established a murine model to accomplish these objectives, using body weight as an indicator of oral mucositis development and evaluating tongue tissues on a cellular and molecular level.

2 | MATERIALS AND METHODS

2.1 | Mice and housing

Male Balb/c mice (8–11 weeks old, 24–27 g) were purchased from the Korea Advanced Institute of Science and Technology (Daejeon, Republic of Korea) and maintained under specific pathogen-free conditions with free access to food and water. In each cage, 4 to 5 mice were housed together. After receiving approval from the Institutional Review Committee for Animal Care and Use of Korea Research Institute of Bioscience and Biotechnology (date of approval: 18 June 2018; KRIBB-AEC-18158), all animal experiments were performed in accordance with the Guide for the Care and Use of Laboratory Animals. All experiments were conducted with 5 mice per group.

2.2 | Establishing the chemoradiation-induced oral mucositis mouse model

On Day 0, mice were administered 100 mg/kg 5-FU (Sigma-Aldrich) or phosphate-buffered saline (PBS; WelGENE Inc.) via intraperitoneal (i.p.) injection. After 30 min, the mice were anesthetized with 2,2,2-tribromoethanol (Sigma-Aldrich) and received 20 Gy using an X-ray irradiator (X-RAD 320). Irradiation was fractionated: 10 Gy × 2 with a 5-min break between fractions. Custom-made lead shields with a thickness of 0.5 cm were used to limit radiation to the head and neck area, with the mice placed in the supine position. The dose rate was 1.8 Gy per minute using 1.5-mm-thick Al filtration (300 kV), and the focus-to-skin distance was 40 cm.

1-Palmitoyl-2-linoleoyl-3-acetyl-rac-glycerol (1 mg/ml; Enzychem Lifesciences Corporation) was emulsified in PBS. Mice were administered 100 or 250 mg/kg body weight PLAG or PBS by oral gavage before 5-FU injection, and then daily at the same time of each day. After ChemoRT, mice were placed on a heated pad to recover and housed in a temperature- and light-controlled environment. Their body weights were recorded daily. As the ChemoRT-treated mice exhibited significant weight loss (approximately 20%) by Day 9, they were sacrificed on that day, and their tongues and blood samples were collected. No animal died before Day 9.

2.3 | Toluidine blue staining and histopathological examination

Tongues harvested on Day 9 were stained for 1 min with 1% toluidine blue (TB; Sigma-Aldrich) in 10% acetic acid (EMSURE), followed

by repeated washing with 10% acetic acid and PBS (Muanza et al., 2005). Macroscopic photographs were obtained from the dorsal view of tongues, and the stained areas were analysed using ImageJ software (National Institutes of Health, Maryland, USA). The analysed numbers were used to calculate the ulceration area percentage (ulcer area/total area × 100%).

2.4 | Measuring the oral mucosa epithelial thickness

On Day 9, the harvested tongues were fixed in 10% neutral buffered formalin for 24 hr, embedded in paraffin, cut into 4-μm-thick sections, and stained with haematoxylin and eosin (H&E). Oral mucosa epithelial thickness was measured by viewing the H&E samples under a light microscope (Olympus). Epithelial thickness was measured from the basal membrane to the epithelial granular layer on the dorsal surface of each tongue section using the linear measurement tool provided in NIS-Elements BR Ver4 (Nikon). The thickness was measured at 20 randomly selected sites in tissue slides, and the mean values (with standard deviation) were calculated (Ryu et al., 2010; Carrard et al., 2008; Zheng et al., 2009).

2.5 | Histopathologic grading of oral mucositis

On Day 9, the H&E-stained tongue slides underwent histopathological grading of oral mucositis, based on a published study (Sunavala-Dossabhoy, Abreo, Timiri Shanmugam, & Caldito, 2015). A clinical pathologist blinded to the mouse's treatment graded the slides as follows: 0 = no radiation injury (normal mucosa), 1 = focal or diffuse alteration of basal cell layer with nuclear atypia and ≤2 dyskeratotic squamous cells, 2 = epithelial thinning (2–4 cell layers) and/or ≥3 dyskeratotic squamous cells in the epithelium, 3a = loss of epithelium without a break in keratinization or the presence of atrophied eosinophilic epithelium, 3b = subepithelial vesicle or bullous formation, and 4 = complete loss of epithelial and keratinized cell layers (ulceration).

2.6 | Immunohistochemical staining

To detect neutrophil infiltration, cytoplasmic translocation of HMGB1, and phosphorylated MLKL in the mouse tongues, the harvested samples were paraffin-embedded, cut into 4-μm-thick sections, and incubated overnight at 4°C with anti-neutrophil antibody (NIMP-R14) (Invitrogen), anti-HMGB1 (Invitrogen) and anti-P-MLKL (Ser345) (Novus Biologicals, NBP2-66953, LLC). HRP-conjugated goat anti-rat IgG (Santa Cruz Biotechnology) and HRP-conjugated rabbit/mouse antibody (Dako) were then added, and the samples were incubated at room temperature for 15 min, followed by visualization with 3-amino-9-ethylcarbazole substrate (Dako). The tissues were then counterstained with 10% Mayer's haematoxylin (Dako), washed, dehydrated and mounted using Crystal Mount (Sigma-Aldrich). Photographic images were obtained of the dorsal surface of the tongue tissues, viewed under a light microscope (Olympus).

2.7 | Enzyme-linked immunosorbent assay

Concentrations of macrophage inflammatory protein 2 (MIP-2; the murine homologue of CXCL8) and IL-6 were measured in serum and tissue extracts. For tissue extracts, the tongues of each mouse were homogenized and lysed in an extraction buffer (20 mM Tris-HCl, pH 7.5, 150 mM NaCl, 1 mM EDTA, 1% Triton X-100 with protease and phosphatase inhibitor cocktails) (Chen et al., 2018). Mouse MIP-2 and IL-6 ELISA kits (BD Bioscience) were used according to the instructions provided by the manufacturer. Optical densities were measured at 450 nm using an ELISA reader (Molecular Devices). Cytokine levels were calculated using a standard curve generated by a curve-fitting program.

2.8 | Western blotting

Mouse serum was used to detect circulating HMGB1 and heat shock protein 90 (Hsp90), another DAMP. Serum (3 μl) was diluted with 72 μl of 1 × SDS sample buffer and heated at 98°C for 5 min (Abdulahad et al., 2011). The samples were then loaded on 10% and 12% SDS-PAGE gels. Antibodies to HMGB1 (Abcam, ab18256) and Hsp90 (Santa Cruz Biotechnology, SC-13119) were used as the primary antibodies. The protein membrane was stained with Ponceau S solution (Sigma-Aldrich) to demonstrate comparable protein loading (Hwang et al., 2014). To detect the necroptosis signalling pathway, the tongues were homogenized and then lysed in RIPA buffer (LPS Solution) containing phosphatase and protease inhibitor cocktails (Sigma-Aldrich). The samples were loaded on 10% SDS-PAGE gels, and the following primary antibodies were applied: phosphorylated (P)-RIP1 (Cell Signaling Technology #31122), RIPK1 (Abcam, ab72139), P-RIP3 (Thr231/Ser232) (CST, #57220), RIPK3 (Santa Cruz Biotechnology, SC-374639), P-MLKL (Ser345) (Novus Biologicals, NBP2-66953), MLKL (Biorbyt LLC; orb32399) and β-actin (CST, 8H10D10). This was followed by addition of secondary anti-rabbit and anti-mouse antibodies (ENZO Life Sciences).

2.9 | RNA isolation and reverse transcription-polymerase chain reaction

To detect IL-6 and MIP-2 at the transcriptional level, total RNA was isolated from the mouse tongues using Tri-RNA Reagent (FAVORGEN Biotech), as specified by the manufacturer's instructions. RNA concentrations and qualities were measured using a NanoDrop device (Eppendorf BioSpectrometer). For cDNA synthesis, 500 ng total RNA was reverse-transcribed using a primer (oligo-dT) and M-MLV reverse transcriptase (Promega). Conventional PCR was subsequently performed using Solg 2 × h-Taq PCR Smart Mix (SolGent) and the Bio-Rad C1000 Touch Thermal Cycler (Bio-Rad
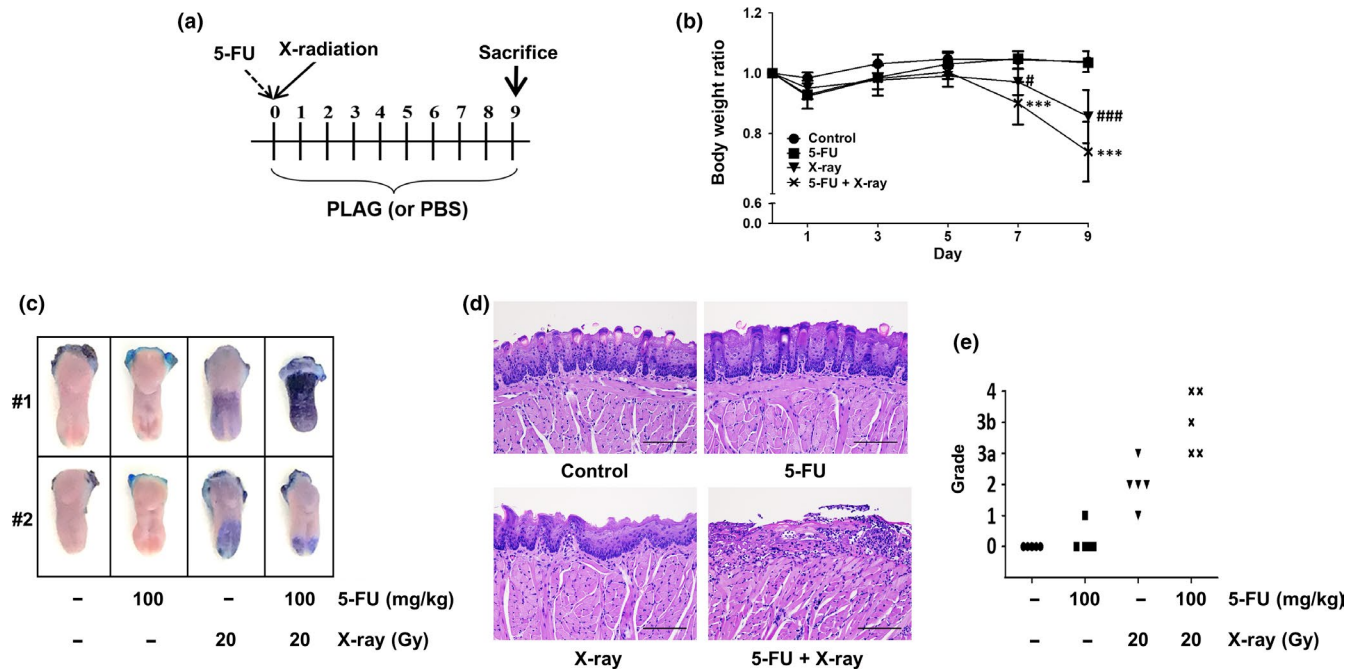
FIGURE 1 Establishment of a chemoradiation-induced oral mucositis mouse model. (a) On Day 0, the mice were divided into different groups. The mice then received 100 mg/kg 5-FU intraperitoneally and 20 Gy X-radiation to the head and neck region. Phosphate-buffered saline (PBS) or PLAG was administered orally each day until Day 9. (b) Changes in body weight were recorded each day and compared between groups. Data are shown as mean ± *SEM* (#*p* < .05, ***p* < .001, ###*p* < .001 vs. Day 0). (c) Mice were sacrificed on Day 9, and their harvested tongues were stained with toluidine blue. (d) Tongues from each treatment group were stained with H&E. Scale bar = 201 µm. (e) Histopathologic grading was determined for each treatment group [Colour figure can be viewed at wileyonlinelibrary.com]

Laboratories). The following MIP-2 and IL-6 primer sets were used: mouse CXCL2 forward, 5′-AGTGAACTGCGCTGTCAATG-3′; mouse CXCL2 reverse, 5′-CTTTGGTTCTTCCTTGAGG-3′; mouse IL-6 forward, 5′-GATGCTACCAAACTGGATA TAATC-3′; and mouse IL-6 reverse, 5′-GGTCCTTAGCCACTCCTTCTGTG-3′.

2.10 | Statistical analysis

Quantitative results are expressed as mean ± standard error of the mean (*SEM*). All statistical analyses were performed using GraphPad Prism, version 5.01 (GraphPad Software Inc.). When comparing serially collected data, two-way repeated measures analysis of variance (ANOVA) was used. When analysing data collected at one time point, one-way ANOVA was used for comparisons between multiple groups, and Student's *t* test was used for comparisons between two experimental groups. *p* values <.05 were considered statistically significant.

3 | RESULTS

3.1 | Establishment of an X-radiation and 5-FU–induced oral mucositis mouse model

Based on previously published reports (Maria, Syme, Eliopoulos, & Muanza, 2016; Ryu et al., 2010; Zhao et al., 2009), we conducted a series of experiments using 5-FU and X-radiation to induce oral

mucositis in a murine model. Accordingly, a chemoradiation-induced oral mucositis mouse model was established with the following doses: 100 mg/kg 5-FU and 20 Gy X-radiation to the head and neck region (Figure 1a). To characterize the model, we evaluated these four groups: control, 20 Gy, 5-FU, and ChemoRT (100 mg/kg 5-FU + 20 Gy X-radiation). Changes in body weight were monitored and recorded daily, as they are an important indicator of the development of mucositis in murine models and human patients (Al Jaouni et al., 2017; Co, Mejia, Que, & Dizon, 2016). Reduced dietary intake and poor absorption of nutrients secondary to difficulties with swallowing or inflammation of oral mucous membranes have been associated with decreased body weight in murine models (Patel, Biswas, Shoja, Ramalingayya, & Nandakumar, 2014). All mice were sacrificed on Day 9 because the ChemoRT-treated mice had lost approximately 20% of their body weight by that time, necessitating euthanasia. As shown in Figure 1b, the 20 Gy and ChemoRT groups exhibited significant weight loss by Day 7, compared to Day 0, and the weight loss was more severe by Day 9 (Day 9 control: 26.50 ± 3.10 g, *p* = .30 vs. Day 0; Day 9 20 Gy: 21.82 ± 0.85 g, *p* < .001 vs. Day 0; Day 9 5-FU: 25.04 ± 2.79 g, *p* = .34 vs. Day 0; Day 9 ChemoRT: 23.62 ± 2.87 g, *p* < .001 vs. Day 0). Figure 1c displays the harvested tongues stained with TB on Day 9. ChemoRT-treated mice exhibited the most severe changes, with prominent ulcers. Figure 1d shows H&E staining of the dorsum of the harvested tongues. Figure 1e illustrates the histopathological grading results for each treatment group. The ChemoRT group had the most severe histopathological changes, with the tongues from all mice graded as 3a or higher.
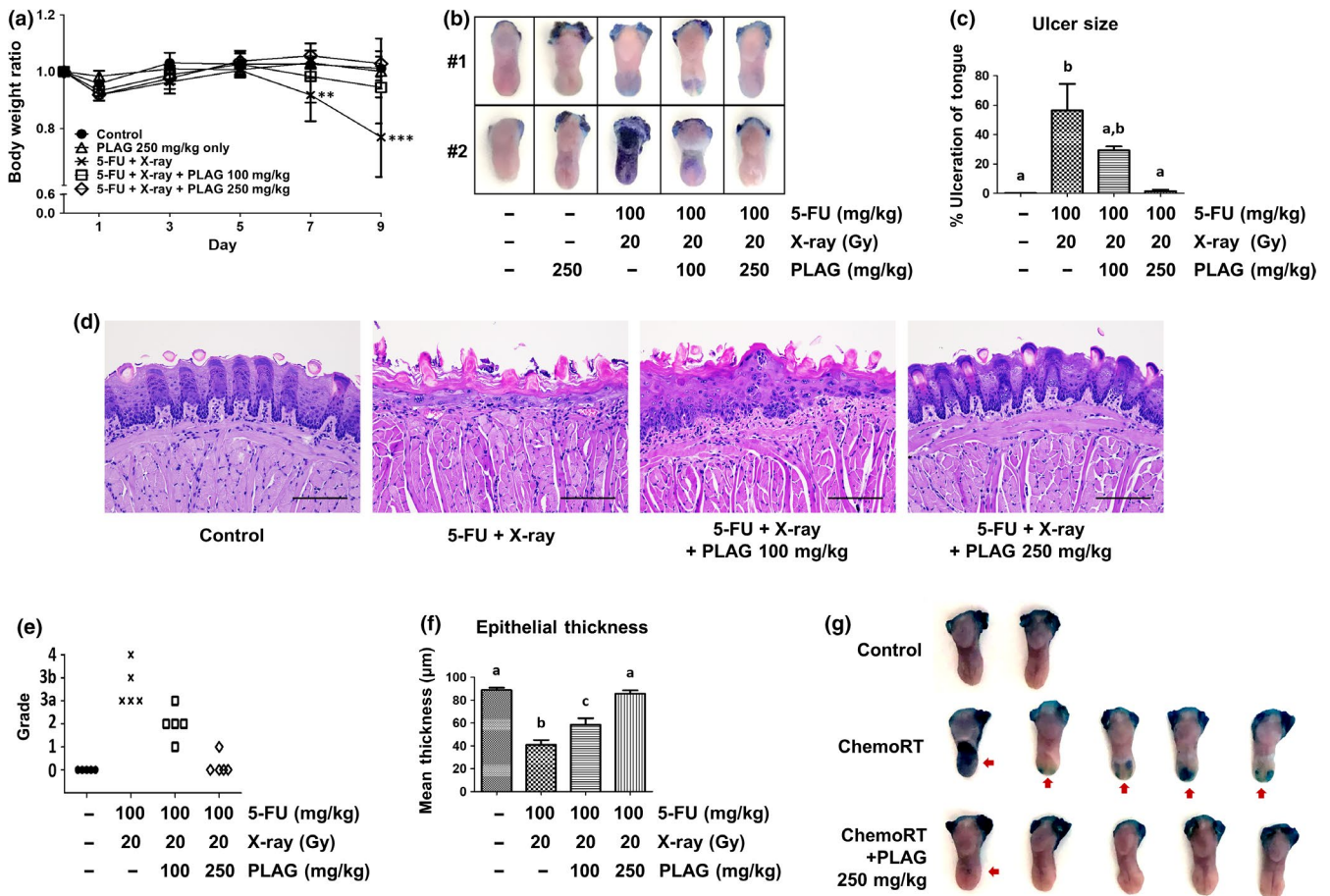
FIGURE 2 1-Palmitoyl-2-linoleoyl-3-acetyl-rac-glycerol (PLAG) attenuated chemoradiation-induced oral mucositis. (a) ChemoRT (100 mg/kg 5-FU and 20 Gy X-radiation) was administered to the mice, with or without the addition of 100 mg/kg or 250 mg/kg PLAG. Body weight was recorded daily. Data are shown as mean ± *SEM* (**p < .01, ***p < .001 vs. Day 0). (b) On Day 9, mice were sacrificed, and the harvested tongues were stained with toluidine blue. (c) Ulcer size was measured using ImageJ, and the ratio of ulcer area/total area was expressed as a percentage. (d) Tongues from each treatment group were stained with H&E. (e) Histopathologic grading was determined for each treatment group. Scale bar = 201 μm. (f) Oral mucosa epithelial thickness was measured at 20 randomly selected sites in tissue slides and compared between groups. (g) The experiment was repeated with ChemoRT and ChemoRT + PLAG 250 mg/kg-treated groups, and the harvested tongues were stained with toluidine blue for comparison. Data represent mean ± *SEM*. Significant differences between groups with *p* < .05 are marked with different letters (a, b and c) [Colour figure can be viewed at wileyonlinelibrary.com]

3.2 | PLAG attenuated chemoradiation-induced oral mucositis

To investigate whether PLAG ameliorates chemoradiation-induced oral mucositis, different doses of PLAG were administered to the mice daily. As shown in Figure 2a, no significant weight loss occurred from Day 0 to Day 9 in control mice or ChemoRT-treated mice who received 100 mg/kg or 250 mg/kg PLAG; by contrast, significant weight loss was observed in the ChemoRT-treated group who did not receive PLAG (Day 9 control: 25.72 ± 1.23 g, *p* = .38 vs. Day 0; Day 9 PLAG only: 25.66 ± 0.70 g, *p* = .35 vs. Day 0; Day 9 ChemoRT: 20.94 ± 2.90 g, *p* < .001 vs. Day 0; Day 9 ChemoRT + PLAG 100 mg/kg: 23.98 ± 2.80 g, *p* = .18 vs. Day 0; Day 9 ChemoRT + PLAG 250 mg/kg: 26.46 ± 1.68 g, *p* = .24 vs. Day 0). Figure 2b displays the harvested tongues stained with TB on Day 9. The ChemoRT group

developed ulcerations and erosions on their tongues, whereas the ChemoRT + PLAG mice exhibited fewer ulcerations.

We used these three markers to assess oral mucositis: ulceration area, histopathologic grading and oral mucosa epithelial thickness. ImageJ analysis showed that the ulceration area percentage was higher in the ChemoRT-treated mice receiving no PLAG than in the control mice (control: 0.17 ± 0.13% and ChemoRT: 56.43 ± 37.89%, *p* < .01). By contrast, the ulceration area percentage was significantly lower in the ChemoRT + 250 mg/kg PLAG group than in the ChemoRT group (ChemoRT + PLAG 100 mg/kg: 29.32 ± 5.40%, *p* = .10 vs. ChemoRT; ChemoRT + PLAG 250 mg/kg: 1.45 ± 2.36%, *p* < .01 vs. ChemoRT) (Figure 2c). H&E staining (Figure 2d) and histopathologic grading (Figure 2e) showed that the tongues of the ChemoRT-treated mice who did not receive PLAG were the most severely injured. The tongues of all 5 mice in the ChemoRT group
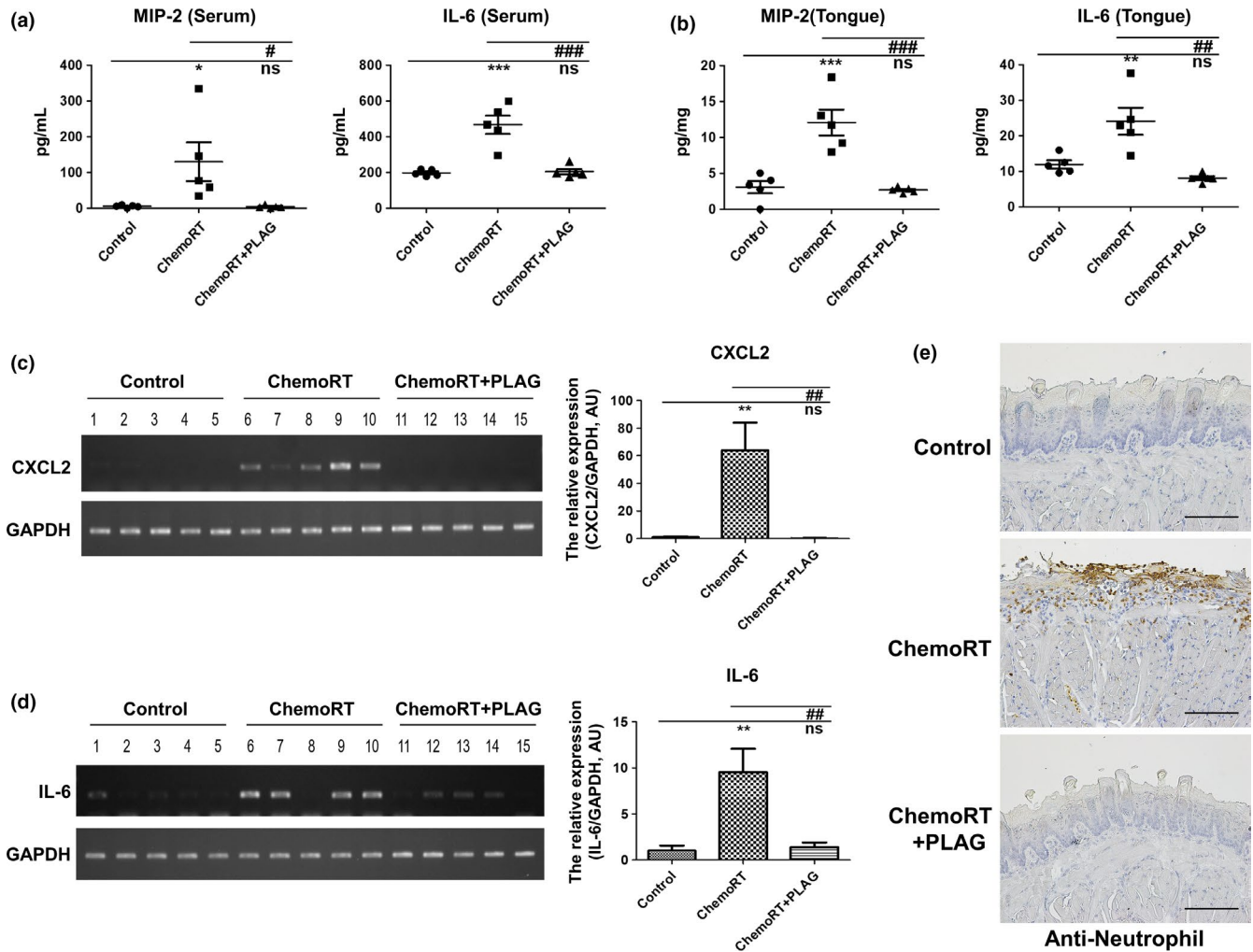
FIGURE 3 1-Palmitoyl-2-linoleoyl-3-acetyl-rac-glycerol (PLAG) ameliorated proinflammatory cytokine release and neutrophil infiltration. (a) Samples obtained from control, ChemoRT (100 mg/kg 5-FU + 20 Gy) and ChemoRT + PLAG 250 mg/kg group mice on Day 9 were used to detect serum levels of the proinflammatory cytokines MIP-2 and IL-6. (b) Tongue extracts were used to detect MIP-2 and IL-6 levels. (c) Expression of MIP-2 (CXCL2) in tongue tissues was examined at the transcriptional level using RT-PCR. Relative expression was compared between groups. (d) IL-6 mRNA expression was detected using RT-PCR, and relative expression was compared between groups. (e) Immunohistochemistry was performed with the neutrophil-specific antibody NIMP-R14. The ChemoRT group displayed neutrophil infiltration in the epithelium, whereas the PLAG co-treated group did not exhibit this infiltration. Neutrophils are stained brown. Scale bar = 201 μm. Data are shown as mean ± *SEM* (*/#*p* < .05, **/##*p* < .01, ***/##*p* < .001) [Colour figure can be viewed at wileyonlinelibrary.com]

were graded as 3a, 3b or 4, whereas the tongues of all ChemoRT-treated mice who received 250 mg/kg PLAG were graded as 0 or 1.

Oral mucosa epithelial thickness was evaluated using H&E-stained tongues (Figure 2f). The ChemoRT group had significantly thinner epithelium than the control group (control: 88.96 ± 9.06 μm and ChemoRT: 41.01 ± 17.82 μm, *p* < .05). PLAG reduced ChemoRT-induced damage, as the epithelial thickness was greater in the ChemoRT-treated mice who received either dose of PLAG than in ChemoRT-treated mice who did not receive PLAG (ChemoRT + PLAG 100 mg/kg: 58.06 ± 24.97 μm, *p* < .05 and ChemoRT + PLAG 250 mg/kg: 85.81 ± 12.24 μm, *p* < .001, compared to the ChemoRT group).

Overall, the higher PLAG dose was associated with most prominent anti-mucositis effects. Therefore, all subsequent experiments were conducted by comparing the ChemoRT group with the ChemoRT + PLAG 250 mg/kg group (Figure 2g).

3.3 | PLAG ameliorated proinflammatory cytokine release and neutrophil infiltration

To determine the effects of oral mucositis on the inflammatory response, serum levels of proinflammatory cytokines were examined by ELISA. Figure 3a shows that on Day 9, the serum levels of both MIP-2 and IL-6 were higher in the ChemoRT group than in the control group (MIP-2 control vs. ChemoRT: 5.57 ± 3.49 pg/ml vs. 130.14 ± 114.54 pg/ml, *p* < .05; IL-6 control vs. ChemoRT: 198.25 ± 16.91 pg/ml vs. 467.25 ± 108.12 pg/ml, *p* < .001). By contrast, ChemoRT-treated mice who received PLAG exhibited substantially less systemic inflammation than ChemoRT-treated mice who did not receive PLAG (MIP-2:4.42 ± 4.04 pg/ml, *p* < .05 vs. ChemoRT; IL-6:205.75 ± 30.41 pg/ml, *p* < .001 vs. ChemoRT).

FIGURE 4 Release of DAMPs
was reduced by PLAG. (a) Levels of
DAMPs in the serum from control,
ChemoRT (100 mg/kg 5-FU + 20 Gy)
and ChemoRT + PLAG 250 mg/kg group
mice were examined by Western blotting.
HMGB1 and Hsp90 were detected in
the serum samples obtained on Day 9.
Ponceau S staining of membrane proteins
was used to demonstrate comparable
protein loading. (b) HMGB1 localization
was observed by immunohistochemistry.
Cytoplasmic HMGB1 was positively
stained in the ChemoRT group. Nuclei are
stained blue; HMGB1 is stained brown.
Scale bars = 201 μm (upper panels) and
40.1 μm (lower panels) [Colour figure can
be viewed at wileyonlinelibrary.com]
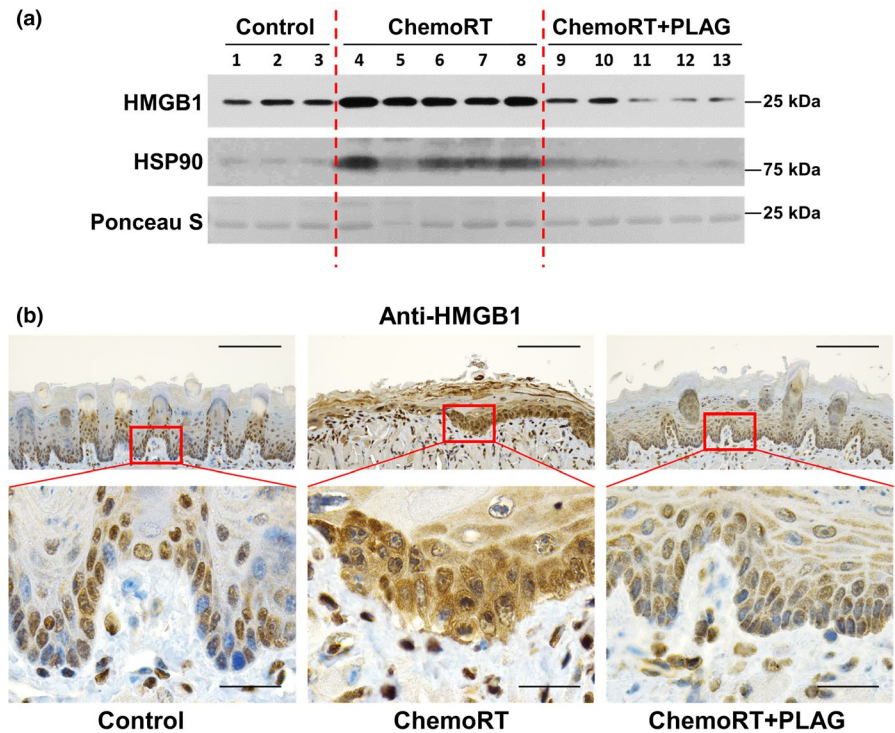
To confirm whether the systemic inflammation in the ChemoRT group was caused by oral mucositis, cytokine levels in tongue-specific protein extracts were also measured. As shown in Figure 3b, the findings were similar to those of the serum samples. MIP-2 and IL-6 levels in tongue tissue extracts were higher in the ChemoRT group than in the control group (MIP-2 control vs. ChemoRT: 3.07 ± 1.78 pg/mg vs. 12.07 ± 3.82 pg/mg, $p < .001$; IL-6 control vs. ChemoRT: 11.97 ± 2.39 pg/mg vs. 24.12 ± 8.01 pg/mg, $p < .01$). By contrast, mice receiving PLAG had lower MIP-2 and IL-6 levels than those undergoing ChemoRT alone (MIP-2:2.69 ± 0.38 pg/mg, $p < .001$ vs. ChemoRT; IL-6:8.13 ± 1.19 pg/mg, $p < .01$ vs. ChemoRT).

CXCL2 expression and IL-6 mRNA expression in the mouse tongues were compared by calculating relative band intensities using ImageJ, with the values expressed in arbitrary units (AU). mRNA expression of both CXCL2 and IL-6 was elevated in the tongues of ChemoRT-treated mice, compared to the control mice (CXCL2 control vs. ChemoRT: 1.00 ± 1.35 AU vs. 64.06 ± 42.00 AU, $p < .01$; IL-6 control vs. ChemoRT: 1.00 ± 1.16 AU vs. 9.55 ± 5.34 AU, $p < .01$). Further, mRNA expression of both cytokines was downregulated in the PLAG group, compared with the ChemoRT (CXCL2: 0.23 ± 0.48 AU, $p < .01$ vs. ChemoRT; IL-6:1.34 ± 1.06 AU, $p < .01$ vs. ChemoRT) (Figure 3c,d).

To detect neutrophil infiltration in the oral epithelium, tissue slides were stained with the anti-neutrophil antibody NIMP-R14 for immunohistochemistry (IHC). The tongues of ChemoRT-treated mice who did not receive PLAG exhibited neutrophil recruitment in the oral epithelium due to elevated levels of MIP-2, whereas neutrophil infiltration was not observed in the tongues of ChemoRT-treated mice who received PLAG (Figure 3e).

3.4 | Release of DAMPs was reduced by PLAG

To further evaluate systemic inflammation and its relation to necrotic epithelium, serum levels of DAMPs were examined by Western blotting. Serum levels of HMGB1 and Hsp90 were higher in the ChemoRT group than in the control group, but the levels of both DAMPs were similar between PLAG-treated and control mice (Figure 4a). To determine whether HMGB1 detected in the serum originated from the oral mucosa, we performed IHC by staining tongue tissue slides with anti-HMGB1 (Im et al., 2019). As shown in Figure 4b, cytoplasmic HMGB1 was positively stained in the ChemoRT group, indicating that translocation of HMGB1 from the nucleus to the cytoplasm occurred in these mice. By contrast, HMGB1 remained in the nucleus in PLAG-treated mice.

3.5 | PLAG downregulates the necroptosis signalling pathway

To assess whether the observed inflammatory responses were associated with necroptotic damage in the oral mucosa, the necroptosis signalling pathway was examined in tongue lysates using Western blotting (Figure 5a). Relative band intensities were determined and compared between groups using Student's t test.

(a)

(b)

(c)

Anti-P-MLKL

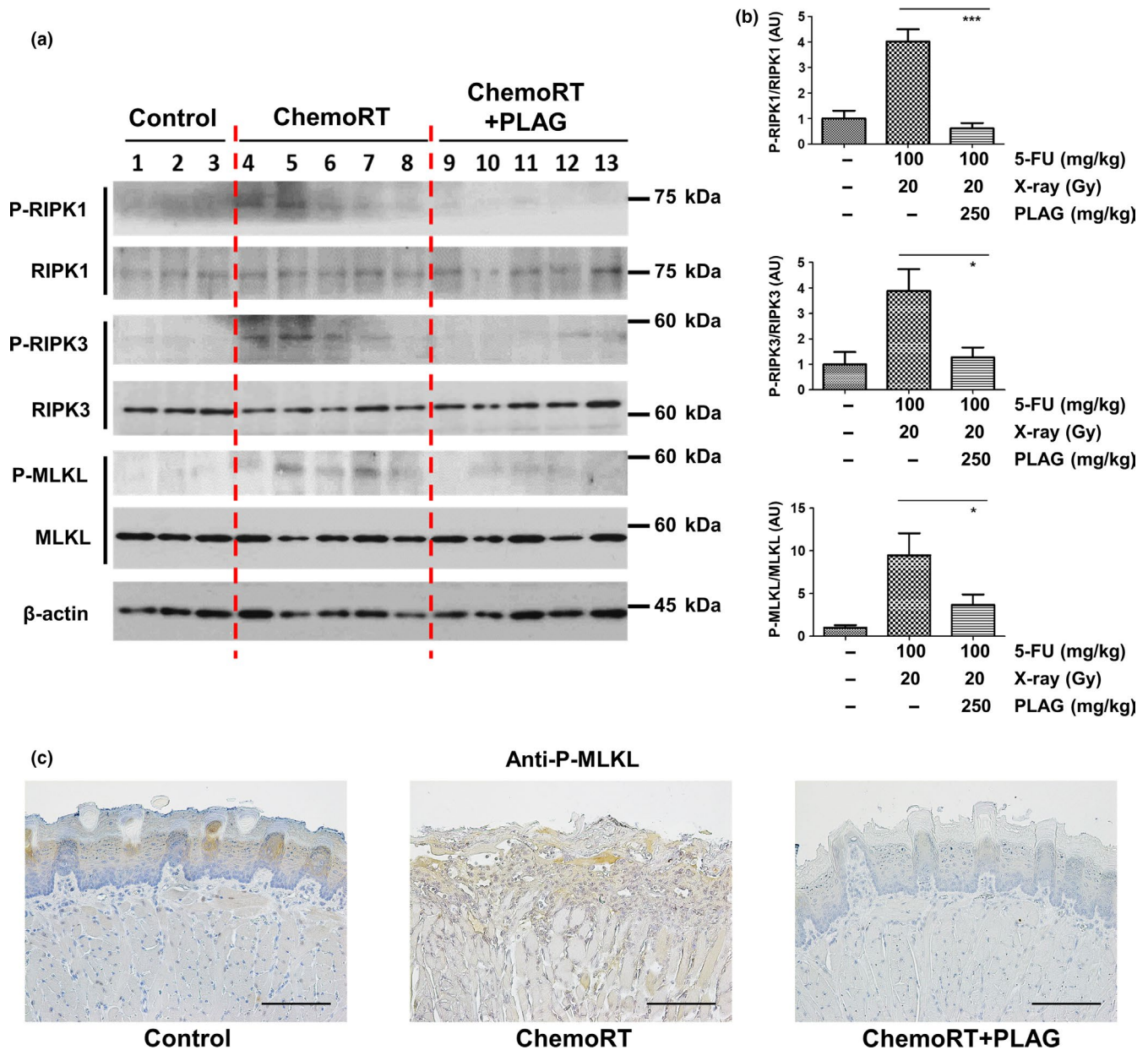Control · ChemoRT · ChemoRT+PLAG

FIGURE 5 PLAG downregulated necroptosis signalling in tongues with chemoradiation-induced oral mucositis. (a) Protein levels of the necroptosis markers RIPK1, RIPK3 and MLKL were detected by Western blotting in tongue lysates from control, ChemoRT (100 mg/ kg 5-FU + 20 Gy) and ChemoRT + PLAG 250 mg/kg groups. (b) Band densities of phosphorylated RIPK1 (P-RIPK1), RIPK3 (P-RIPK3) and MLKL (P-MLKL) were compared to band densities of total RIPK1, RIPK3 and MLKL using ImageJ. (c) P-MLKL was visualized by immunohistochemistry. P-MLKL is stained brown. Scale bar = 201 μm. Data are shown as mean ± *SEM* (*$p < .05$, ***$p < .001$ vs. ChemoRT using Student's *t* test) [Colour figure can be viewed at wileyonlinelibrary.com]

The results showed that phosphorylation of RIPK1, RIPK3 and MLKL in the tongues of ChemoRT-treated mice was modulated by PLAG (P-RIPK1 control vs. ChemoRT vs. ChemoRT + PLAG: 1.00 ± 0.45 AU vs. 4.02 ± 1.02 AU vs. 0.61 ± 0.45 AU, $p < .01$ for ChemoRT vs. ChemoRT + PLAG; P-RIPK3 control vs. ChemoRT vs. ChemoRT + PLAG: 1.00 ± 0.74 AU vs. 3.88 ± 1.81 AU vs. 1.27 ± 0.83 AU, $p < .05$ for ChemoRT vs. ChemoRT + PLAG; P-MLKL control vs. ChemoRT vs. ChemoRT + PLAG: 1.00 ± 0.47 AU vs. 9.48 ± 5.45 AU vs. 3.67 ± 2.56 AU, $p < .05$ for ChemoRT vs. ChemoRT + PLAG) (Figure 5b). These findings were verified by histological observations

using IHC. Levels of P-MLKL in the oral mucosa epithelium and connective tissues were higher in the ChemoRT group than in the control and PLAG-treated groups (Figure 5c).

4 | DISCUSSION

Based on our results, we propose a schematic for the pathogenesis of chemoradiation-induced oral mucositis and the role of PLAG (Figure 6). By Day 9 after ChemoRT, mice exhibited oral mucositis
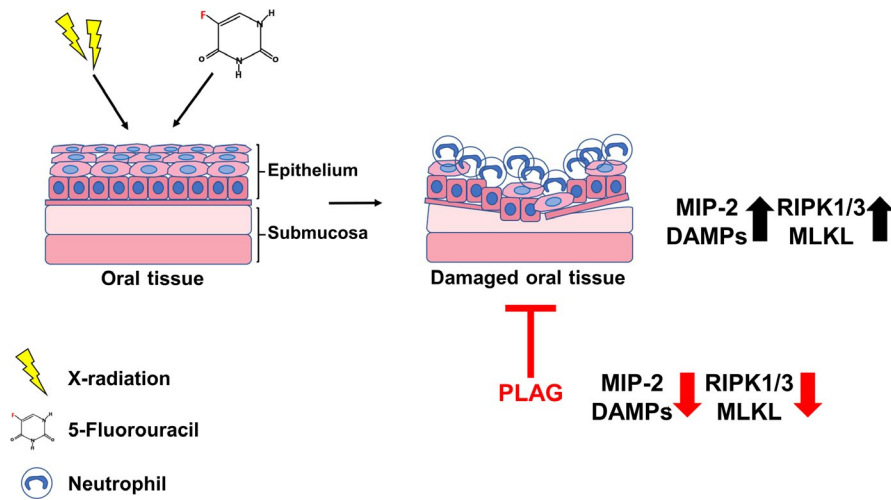
FIGURE 6 Proposed schematic for the pathogenesis of chemoradiation-induced oral mucositis and the role of PLAG. Mice underwent intraperitoneal injection of 5-FU and head and neck X-irradiation. Chemoradiotherapy induced higher than normal levels of proinflammatory cytokines and DAMPs in the oral mucosa and serum. Accordingly, neutrophil infiltration in the oral epithelium was observed, and necroptosis signalling was activated in the tongues. By contrast, PLAG-treated mice had reduced DAMPs and cytokine levels by Day 9, which were similar to those of control mice who did not undergo chemoradiation. Furthermore, activation of the necroptosis signalling pathway (RIPK1, RIPK3 and MLKL axis) was reduced by PLAG treatment, protecting oral mucosa tissues from chemoradiation-induced damage [Colour figure can be viewed at wileyonlinelibrary.com]

as an acute response. DAMPs and proinflammatory cytokines were released from the damaged oral mucosa and led to systemic necro-inflammation via the circulatory system. In addition, neutrophils were recruited to the oral epithelium because of the elevated MIP-2 level and passively released DAMPs. Tongue tissues from ChemoRT-treated mice also exhibited activation of the necroptotic signalling axis, confirming that the inflammatory response was related to necroptosis. We also confirmed that PLAG ameliorated oral mucositis by lowering levels of proinflammatory cytokines and DAMPs through modulation of the necroptosis signalling pathway.

Effective early management of necroptosis is critical, as necroptosis can cause systemic inflammation, leading to damage in other tissues and thereby increasing the difficulty of successful treatment. During necroptosis of injured tissues (as can be induced by chemotherapy or radiotherapy), neutrophils are recruited to eliminate DAMPs that may threaten normal tissues via autocrine and paracrine effects (Watts & Walmsley, 2018; Pouwels et al., 2016; Buisan et al., 2017; Handly, Pilko, & Wollman, 2015; Choi, Cui, Chowdhury, & Kim,2017). The level of neutrophil recruitment at the site of oral lesions in mucositis correlates with the severity of histological changes, including ulceration (Barbosa et al., 2018a; Lopes et al., 2010). Increased oral neutrophil infiltration is especially prominent in 5-FU-induced oral mucositis (Barbosa et al., 2018b; Wright, Meierovics, & Foxley, 1986).

In addition to symptomatic treatment with analgesics and antibiotics for secondary infection, other treatment options currently available for oral mucositis include synthetic glucocorticoids (e.g. dexamethasone) and recombinant human keratinocyte growth factor (palifermin) (Lalla et al., 2014). Dexamethasone functions primarily as an immunosuppressive agent, and palifermin stimulates epithelial cell proliferation. These two medications must be utilized with much consideration of the dosage and duration of treatment to prevent side effects and tumour cell growth (Riley et al., 2017). PLAG may be another potential preventive or treatment option for oral mucositis, providing a different treatment perspective by regulating necroptosis and the positive feedback loops involving DAMPs and proinflammatory cytokines.

Our results have shown that PLAG may have preventive activity against chemoradiation-induced oral mucositis, a common side effect of head and neck cancer therapy. Although no published studies have directly examined the relationship between head and neck cancer therapy and PLAG, a recent study evaluated the effects of PLAG on gemcitabine-induced neutropenia in a mice model (Jeong et al., 2019). According to that study, PLAG attenuated the neutropenia and did not interfere with the anti-cancer effect of gemcitabine in athymic nude mice implanted with a human myeloma cell line. Therefore, we expect that PLAG may ameliorate oral mucositis caused by cancer therapy without interfering with treatment efficacy in patients with head and neck cancer.

In conclusion, chemoradiotherapy led to necroptosis of the tongue by Day 9 in our mouse model. Release of DAMPs and proinflammatory cytokines from oral mucosa cells and subsequent neutrophil infiltration into the oral epithelium were observed. PLAG ameliorated chemoradiation-induced oral mucositis by modulating the necroptosis signalling pathway. Based on these observations, we suggest that PLAG may be a useful option for preventing or treating chemoradiation-induced oral mucositis.

CONFLICTS OF INTEREST

The authors have no conflicts of interest.

AUTHOR CONTRIBUTIONS

SC conducted the experiments, analysed the data, and wrote the manuscript. S-HS developed the methodology and acquired the data. H-RL designed the study and developed the methodology. K-YS provided the materials and analysed the data. SY reviewed and revised the manuscript. JWK supervised the study and analysed and interpreted the data.

ORCID

Jae Wha Kim iD https://orcid.org/0000-0002-1507-2731

REFERENCES

Abdulahad, D. A., Westra, J., Bijzet, J., Limburg, P. C., Kallenberg, C. G., & Bijl, M. (2011). High mobility group box 1 (HMGB1) and anti-HMGB1 antibodies and their relation to disease characteristics in systemic lupus erythematosus. *Arthritis Research & Therapy*, *13*, R71.

Al Jaouni, S. K., Al Muhayawi, M. S., Hussein, A., Elfiki, I., Al-Raddadi, R., Al Muhayawi, S. M., ... Harakeh, S. (2017). Effects of honey on oral mucositis among pediatric cancer patients undergoing chemo/radiotherapy treatment at King Abdulaziz University Hospital in Jeddah, Kingdom of Saudi Arabia. *Evidence-based Complementary and Alternative Medicine*, *2017*, 5861024.

Al-Dasooqi, N., Sonis, S. T., Bowen, J. M., Bateman, E., Blijlevens, N., Gibson, R. J. ... Mucositis Study Group of the Multinational Association of Supportive Care in Cancer/International Society of Oral O (2013). Emerging evidence on the pathobiology of mucositis. *Supportive Care in Cancer*, *21*, 3233–3241.

Barbosa, L. A., Fiuza, P. P., Borges, L. J., Rolim, F. A., Andrade, M. B., Luz, N. F., ... Prates, D. B. (2018a). RIPK1-RIPK3-MLKL-associated necroptosis drives *Leishmania infantum* killing in neutrophils. *Frontiers in Immunology*, *9*, 1818.

Barbosa, M. M., de Araujo, A. A., de Araujo Junior, R. F., Guerra, G. C. B., de Castro Brito, G. A., Leitao, R. C., ... de Medeiros, C. (2018b). Telmisartan Modulates the Oral Mucositis Induced by 5-Fluorouracil in Hamsters. *Frontiers in physiology*, *9*, 1204.

Bertolini, M., Sobue, T., Thompson, A., & Dongari-Bagtzoglou, A. (2017). Chemotherapy induces oral mucositis in mice without additional noxious stimuli. *Translational Oncology*, *10*, 612–620.

Buisan, O., Orsola, A., Oliveira, M., Martinez, R., Etxaniz, O., Areal, J., & Ibarz, L. (2017). Role of Inflammation in the Perioperative Management of Urothelial Bladder Cancer With Squamous-Cell Features: Impact of Neutrophil-to-Lymphocyte Ratio on Outcomes and Response to Neoadjuvant Chemotherapy. *Clinical Genitourinary Cancer*, *15*, e697–e706.

Carrard, V. C., Pires, A. S., Badauy, C. M., Rados, P. V., Lauxen, I. S., & Sant'Ana Filho, M. (2008). Effects of aging on mouse tongue epithelium focusing on cell proliferation rate and morphological aspects. *The Bulletin of Tokyo Dental College*, *49*, 199–205.

Chen, W., Kang, K. L., Alshaikh, A., Varma, S., Lin, Y. L., Shin, K. H., ... Kang, M. K. (2018). Grainyhead-like 2 (GRHL2) knockout abolishes oral cancer development through reciprocal regulation of the MAP kinase and TGF-beta signaling pathways. *Oncogenesis*, *7*, 38.

Choi, J. Y., Cui, Y., Chowdhury, S. T., & Kim, B. G. (2017). High-mobility group box-1 as an autocrine trophic factor in white matter stroke.

Proceedings of the National Academy of Sciences of the United States of America, *114*, E4987–E4995.

Cinausero, M., Aprile, G., Ermacora, P., Basile, D., Vitale, M. G., Fanotto, V., ... Sonis, S. T. (2017). New frontiers in the pathobiology and treatment of cancer regimen-related mucosal injury. *Frontiers in Pharmacology*, *8*, 354.

Co, J. L., Mejia, M. B., Que, J. C., & Dizon, J. M. (2016). Effectiveness of honey on radiation-induced oral mucositis, time to mucositis, weight loss, and treatment interruptions among patients with head and neck malignancies: A meta-analysis and systematic review of literature. *Head & Neck*, *38*, 1119–1128.

Deepa, S. S., Unnikrishnan, A., Matyi, S., Hadad, N., & Richardson, A. (2018). Necroptosis increases with age and is reduced by dietary restriction. *Aging Cell*, *17*, e12770.

de Oliveira, S., Reyes-Aldasoro, C. C., Candel, S., Renshaw, S. A., Mulero, V., & Calado, A. (2013). Cxcl8 (IL-8) mediates neutrophil recruitment and behavior in the zebrafish inflammatory response. *Journal of Immunology*, *190*, 4349–4359.

Handly, L. N., Pilko, A., & Wollman, R. (2015). Paracrine communication maximizes cellular response fidelity in wound signaling. *ELife*, *4*, e09652.

He, H. G., Zhu, L., Li, H. C., Wang, W., Vehvilainen-Julkunen, K., & Chan, S. W. (2014). A randomized controlled trial of the effectiveness of a therapeutic play intervention on outcomes of children undergoing inpatient elective surgery: Study protocol. *Journal of Advanced Nursing*, *70*, 431–442.

Hwang, H. J., Sohn, K. Y., Han, Y. H., Chong, S., Yoon, S. Y., Kim, Y. J., ... Kim, J. W. (2015). Effect of 1-palmitoyl-2-linoleoyl-3-acetyl-rac-glycerol on immune functions in healthy adults in a randomized controlled trial. *Immune Network*, *15*, 150–160.

Hwang, J. S., Lee, W. J., Kang, E. S., Ham, S. A., Yoo, T., Paek, K. S., ... Seo, H. G. (2014). Ligand-activated peroxisome proliferator-activated receptor-delta and -gamma inhibit lipopolysaccharide-primed release of high mobility group box 1 through upregulation of SIRT1. *Cell Death & Disease*, *5*, e1432.

Im, K. I., Nam, Y. S., Kim, N., Song, Y., Lee, E. S., Lim, J. Y., ... Cho, S. G. (2019). Regulation of HMGB1 release protects chemoradiotherapy-associated mucositis. *Mucosal Immunology*, *12*:1070–1081.

Jeong, J., Kim, Y. J., Lee, D. Y., Moon, B. G., Sohn, K. Y., Yoon, S. Y., & Kim, J. W. (2019). 1-Palmitoyl-2-linoleoyl-3-acetyl-rac-glycerol (PLAG) attenuates gemcitabine-induced neutrophil extravasation. *Cell & Bioscience*, *9*, 4.

Jeong, J., Kim, Y. J., Yoon, S. Y., Kim, Y. J., Kim, J. H., Sohn, K. Y., ... Kim, J. W. (2016). PLAG (1-Palmitoyl-2-Linoleoyl-3-Acetyl-rac-Glycerol) modulates eosinophil chemotaxis by regulating CCL26 expression from epithelial cells. *PLoS ONE*, *11*, e0151758.

Kaczmarek, A., Vandenabeele, P., & Krysko, D. V. (2013). Necroptosis: The release of damage-associated molecular patterns and its physiological relevance. *Immunity*, *38*, 209–223.

Kim, Y. J., Shin, J. M., Shin, S. H., Kim, J. H., Sohn, K. Y., Kim, H. J., ... Kim, J. W. (2017). 1-palmitoyl-2-linoleoyl-3-acetyl-rac-glycerol ameliorates arthritic joints through reducing neutrophil infiltration mediated by IL-6/STAT3 and MIP-2 activation. *Oncotarget*, *8*, 96636–96648.

Ko, Y. E., Yoon, S. Y., Ly, S. Y., Kim, J. H., Sohn, K. Y., & Kim, J. W. (2018). 1-palmitoyl-2-linoleoyl-3-acetyl-rac-glycerol (PLAG) reduces hepatic injury in concanavalin A-treated mice. *Journal of Cellular Biochemistry*, *119*, 1392–1405.

Lalla, R. V., Bowen, J., Barasch, A., Elting, L., Epstein, J., Keefe, D. M., ... Mucositis Guidelines Leadership Group of the Multinational Association of Supportive Care in C and International Society of Oral O (2014). MASCC/ISOO clinical practice guidelines for the management of mucositis secondary to cancer therapy. *Cancer*, *120*, 1453–1461.

Lee, H. R., Yoo, N., Kim, J. H., Sohn, K. Y., Kim, H. J., Kim, M. H., ... Kim, J. W. (2016). The therapeutic effect of PLAG against oral mucositis in hamster and mouse model. *Frontiers in Oncology*, *6*, 209.

Liu, C., Zhang, K., Shen, H., Yao, X., Sun, Q., & Chen, G. (2018). Necroptosis: A novel manner of cell death, associated with stroke (Review). *International Journal of Molecular Medicine*, *41*, 624–630.

Lopes, N. N., Plapler, H., Lalla, R. V., Chavantes, M. C., Yoshimura, E. M., da Silva, M. A., & Alves, M. T. (2010). Effects of low-level laser therapy on collagen expression and neutrophil infiltrate in 5-fluorouracil-induced oral mucositis in hamsters. *Lasers in Surgery and Medicine*, *42*, 546–52.

Maria, O. M., Eliopoulos, N., & Muanza, T. (2017). Radiation-induced oral mucositis. *Frontiers in Oncology*, *7*, 89.

Maria, O. M., Syme, A., Eliopoulos, N., & Muanza, T. (2016). Single-dose radiation-induced oral mucositis mouse model. *Frontiers in Oncology*, *6*, 154.

Muanza, T. M., Cotrim, A. P., McAuliffe, M., Sowers, A. L., Baum, B. J., Cook, J. A., … Mitchell, J. B. (2005). Evaluation of radiation-induced oral mucositis by optical coherence tomography. *Clinical Cancer Research*, *11*, 5121–5127.

Patel, A., Biswas, S., Shoja, M. H., Ramalingayya, G. V., & Nandakumar, K. (2014). Protective effects of aqueous extract of *Solanum nigrum* Linn. leaves in rat models of oral mucositis. *The Scientific World Journal*, *2014*, 345939.

Pouwels, S. D., Zijlstra, G. J., van der Toorn, M., Hesse, L., Gras, R., Ten Hacken, N. H.,&… Nawijn, M. C. (2016). Cigarette smoke-induced necroptosis and DAMP release trigger neutrophilic airway inflammation in mice. American journal of physiology. *Lung Cellular and Molecular Physiology*, *310*, L377–86.

Riley, P., Glenny, A. M., Worthington, H. V., Littlewood, A., Fernandez Mauleffinch, L. M., Clarkson, J. E., & McCabe, M. G. (2017). Interventions for preventing oral mucositis in patients with cancer receiving treatment: Cytokines and growth factors. *The Cochrane Database of Systematic Reviews*, *11*, CD011990.

Ryu, S. H., Kang, K. M., Moon, S. Y., Chai, G. Y., Hong, J. P., Cho, K. O., … Lee, S. W. (2010). Therapeutic effects of recombinant human epidermal growth factor (rhEGF) in a murine model of concurrent chemo- and radiotherapy-induced oral mucositis. *Journal of Radiation Research*, *51*, 595–601.

Sottili, M., Mangoni, M., Gerini, C., Salvatore, G., Castiglione, F., Desideri, I., … Livi, L. (2018). Peroxisome proliferator activated receptor-gamma stimulation for prevention of 5-fluorouracil-induced oral mucositis in mice. *Head & Neck*, *40*, 577–583.

Sunavala-Dossabhoy, G., Abreo, F., Timiri Shanmugam, P. S., & Caldito, G. (2015). Histopathologic grading of oral mucositis. *Oral Diseases*, *21*, 355–360.

Tancharoen, S., Shakya, P., Narkpinit, S., Dararat, P., & Kikuchi, K. (2018). Anthocyanins extracted from *Oryza sativa* L. prevent fluorouracil-induced nuclear factor-kappaB activation in oral mucositis. In Vitro and In Vivo Studies. *International Journal of Molecular Sciences*, *19*, E2981.

Vasconcelos, R. M., Sanfilippo, N., Paster, B. J., Kerr, A. R., Li, Y., Ramalho, L., … Corby, P. M. (2016). Host-microbiome cross-talk in oral mucositis. *Journal of Dental Research*, *95*, 725–733.

Watts, E. R., & Walmsley, S. R. (2018). Getting DAMP(s) Wets the Whistle for Neutrophil Recruitment. *Immunity*, *48*, 846–848.

Wright, D. G., Meierovics, A. I., & Foxley, J. M. (1986). Assessing the delivery of neutrophils to tissues in neutropenia. *Blood*, *67*, 1023–30.

Xu, Y., Ma, H., Shao, J., Wu, J., Zhou, L., Zhang, Z., … Han, J. (2015). A role for tubular necroptosis in cisplatin-induced AKI. *Journal of the American Society of Nephrology*, *26*, 2647–2658.

Zhang, Q., Nguyen, A. L., Shi, S., Hill, C., Wilder-Smith, P., Krasieva, T. B., & Le, A. D. (2012). Three-dimensional spheroid culture of human gingiva-derived mesenchymal stem cells enhances mitigation of chemotherapy-induced oral mucositis. *Stem Cells and Development*, *21*, 937–947.

Zhao, H., Jaffer, T., Eguchi, S., Wang, Z., Linkermann, A., & Ma, D. (2015). Role of necroptosis in the pathogenesis of solid organ injury. *Cell Death & Disease*, *6*, e1975.

Zhao, J., Kim, K. A., De Vera, J., Palencia, S., Wagle, M., & Abo, A. (2009). R-Spondin1 protects mice from chemotherapy or radiation-induced oral mucositis through the canonical Wnt/beta-catenin pathway. *Proceedings of the National Academy of Sciences of the United States of America*, *106*, 2331–2336.

Zheng, C., Cotrim, A. P., Sunshine, A. N., Sugito, T., Liu, L., Sowers, A., Mitchell, J. B., & Baum, B. J. (2009). Prevention of radiation-induced oral mucositis after adenoviral vector-mediated transfer of the keratinocyte growth factor cDNA to mouse submandibular glands. *Clinical Cancer Research : An Official Journal of The American Association for Cancer Research*, *15*, 4641–4648.

Zhu, K., Liang, W., Ma, Z., Xu, D., Cao, S., Lu, X., Liu, N., Shan, B., Qian, L., & Yuan, J. (2018). Necroptosis promotes cell-autonomous activation of proinflammatory cytokine gene expression. *Cell Death & Disease*, *9*, 500.